Cent. Eur. J. Phys. • 9(6) • 2011 • 1446-1451
DOI: 10.2478/s11534-011-0063-y

VERSITA

Central European Journal of **Physics**

Co doped ZnO semiconductor materials: structural, morphological and magnetic properties

Research Article

Adriana Popa[1]*, Dana Toloman[1], Oana Raita[1], Alexandru Radu Biris[1], Gheorghe Borodi[1], Thikra Mustafa[2], Fumiya Watanabe[2], Alexandru Sorin Biris[2], Alexandru Darabont[1], Liviu Mihail Giurgiu[1]

1 *National Institute for Research and Development of Isotopic and Molecular Technologies 400293 Cluj-Napoca, P. O. Box 700, Romania*

2 *UALR Nanotechnology Center, Applied Science Department, University of Arkansas at Little Rock, Arkansas, 72204, United States*

Received 10 January 2011; accepted 21 June 2011

Abstract: Structural, morphological and magnetic properties of $Zn_{1-x}Co_xO$ ($x = 0.01$ and 0.03) powdered materials are presented. XRD studies reveal a wurtzite-type structure, while the formation of a Co_3O_4 secondary phase was evidenced by Raman spectroscopy. A ferromagnetic behaviour with low Curie temperature was evidenced by Electron Paramagnetic Resonance (EPR) investigation. We suggest that the origin of the ferromagnetism in $Zn_{1-x}Co_xO$ powders is probably due to the presence of the mixed cation valence of Co ions via a double-exchange mechanism rather than the real doping effect.

PACS (2008): 75.50.Pp, 61.05.cp, 68.37.Hk, 76.50.+g

Keywords: diluted magnetic semiconductors • ZnO powders • ferromagnetism

1. Introduction

In the last decade, due to the perspectives opened by spintronics in the field of information technology and electronics, many experimental and theoretical studies were focused on spin polarized materials, such as diluted magnetic semiconductors (DMS) with Curie temperature above room temperature which permit *n* or *p* doping [1, 2].

Fundamental studies were performed in order to fully understand and elucidate the complex structural, magnetic and electrical properties of the micro- and nanostructured systems based on TiO_2, SnO and ZnO materials doped with 3d transition metals magnetic ions (TM=Mn, Fe, Co) [3, 4, 5]. The experimental data reported for $Zn_{1-x}TM_xO$ by different groups are still rather contradictory. While many groups report room temperature ferromagnetism for the Co doped ZnO [6, 7], there are other studies reporting the absence of ferromagnetism [8, 9]. This suggests that the properties of these materials are most probably highly process dependent and are influenced by the synthesis conditions, crystalline structure, magnetic clustering, doping degree and dimensionality.

Different explanations of the ferromagnetism's (FM) origin were given. For ZnO:TM, hole-mediated ferromagnetism was originally suggested [10]. Recent theoretical models explain ferromagnetic coupling in terms of

*E-mail: popa@itim-cj.ro

bound magnetic polarons [11, 12] or a ligand-to-metal charge transfer [13, 14]. A large number of experimental studies seem to provide evidence for carrier-mediated RT ferromagnetism in ZnO:TM [15, 16]. Recent reports starting from the fact that TM-doped ZnO is known to form nanosized (inter)metallic inclusions [17–20], consider these inclusions responsible for the observed magnetic response [21].

Therefore, continuous efforts are necessary in order to gain a deeper understanding of the origin of ferromagnetism, specific mechanisms, as well as the influence of the dopants distribution and size reduction on the overall spin properties.

The presence of high temperature ferromagnetism, a new phenomenon for $Zn_{1-x}TM_xO$ micro- and nanostructures, represents a necessary condition for the achievement and miniaturization of spintronic devices which could work at ambient temperature.

This work presents a thorough investigation of $Zn_{1-x}Co_xO$ ($x = 0.01$ and 0.03) powders by different techniques such as X ray diffraction (XRD), Raman spectroscopy, Scanning Electron Microscopy (SEM), Energy Dispersive X-ray spectroscopy (EDS), and Electron Paramagnetic Resonance (EPR) spectroscopy in order to understand the structural and magnetic properties of the samples. Such structures could find a number of applications in areas ranging from electronics, spintronics, data storage devices, energy generation processes and areas that require materials with multi-functional properties.

2. Experiment

A series of microcrystalline powders of Co^{2+}-doped ZnO having the general formula $Zn_{1-x}Co_xO$ ($x = 0.01$ and 0.03) were prepared as follows. Stoichiometric amounts of zinc acetate dihydrate $Zn(CH_3COO)_2{\cdot}2H_2O$ (98%) and cobalt acetate tetrahydrate $Co(CH_3COO)_2{\cdot}4H_2O$ were dissolved in distilled water and stirred until a homogenous solution was obtained. The homogeneous solution was then decomposed at 523 K in air until completely dried and the temperature was gradually raised over 2 – 3 days. Prior to the heat treatment the resulting mass precursor was formed into a fine powder. Fractions of these powders were calcinated at 873 K for 2 hours in air.

The phase and morphology of the materials were investigated by various analytical tools such as XRD, SEM and Raman spectroscopy, and the magnetic properties by EPR technique.

X ray diffraction measurement was made using a high resolution Bruker D8 Advance diffractometer with Cu x-ray tube and incident beam Ge (111) monochromator ($\lambda = 1.54056$ Å).

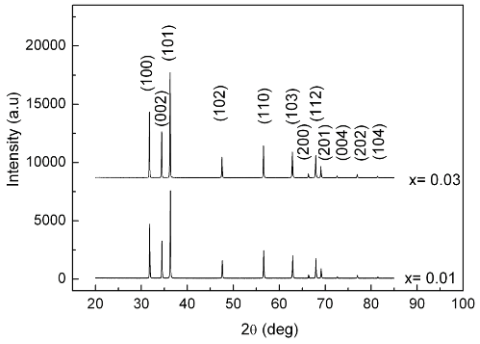

Figure 1. XRD pattern of $Zn_{1-x}Co_xO$ ($x = 0.01$ and 0.03) powders.

Scanning electron microscopy (SEM) analysis was carried out with a JEOL7000F microscope with a specific resolution of 1.2 nm. Energy dispersive x-ray spectroscopy (EDS) was performed using the EDAX system.

The Raman spectra were collected at room temperature using a JASCO NRS-3300 micro-Raman Spectrometer with an air cooled CCD detector in a backscattering geometry and using a 600/mm grating. The microscope objective used for the studies was 100X. As an excitation source, a 785 nm laser line was used, with the power at the sample surface being 85 mW.

X-band Electron Paramagnetic Resonance (EPR) measurements of powder samples were carried out in the 4 – 300 K temperature range using a Bruker E-500 ELEXSYS spectrometer. The spectra processing was performed by Bruker Xepr software.

3. Results and discussion

X-ray powder diffraction (XRD) was used to analyze the structural properties of the materials and to identify the phase and the purity of all the samples. Fig. 1 presents the X-ray powder diffraction pattern recorded for the samples with $x = 0.01$ and 0.03.

Results of XRD measurements indicated that all $Zn_{1-x}Co_xO$ samples have a wurtzite type structure with the lattice parameter $a = b = 3.251$ Å, $c = 5.2055$ Å for $x = 0.01$ and $a = b = 3.249$ Å, $c = 5.205$ Å for $x = 0.03$. No additional peaks except that for ZnO were observed, thus indicating that Co atoms were successfully doped into the lattice of ZnO.

The particles' size and morphology were characterized by SEM microscopy. The images of $Zn_{1-x}Co_xO$ ($x = 0.01$ and

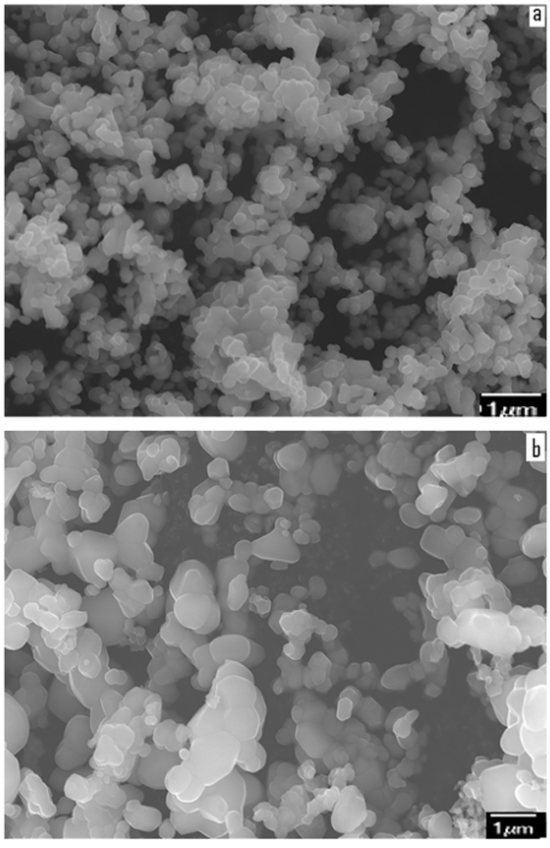

Figure 2. SEM images of $Zn_{1-x}Co_xO$ a) $x = 0.01$, b) $x = 0.03$.

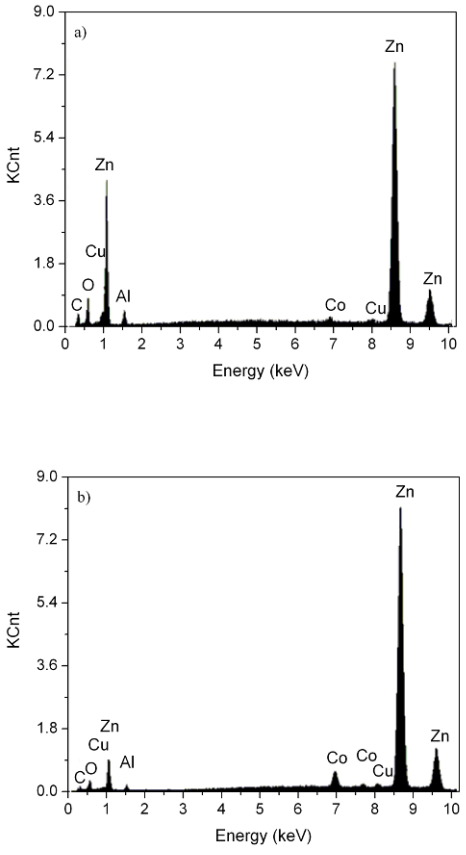

Figure 3. EDS data of $Zn_{1-x}Co_xO$ with a) $x = 0.01$, b) $x = 0.03$.

0.03) are shown in Fig. 2. It was observed that the individual particles have almost spherical shape with a mean size of 170 nm for $x = 0.01$ and 340 nm for $x = 0.03$. However an inherent agglomeration of the individual particles was also noticed.

Elemental analysis of samples has been done using EDS spectroscopy. The existence of the elements which are expected was proved. Alongside the lines of the elements Zn and O (and the lines of the experimental setup elements: Cu, Al), a low intensity signal of Co also appeared in EDS spectra. In addition, an increase in the relative intensity of the Co peaks with increasing x was seen, confirming the progressive incorporation of Co (Fig. 3).

In order to confirm the structures of analysed materials, Raman scattering was performed, as this technique is very sensitive to the microstructure of nanocrystalline materials. In Fig. 4 the Raman spectra at room temperature for $Zn_{1-x}Co_xO$ ($x = 0.01$, 0.03) and pure ZnO powder collected at room temperature are shown.

For the pure ZnO sample, three major peaks are observed. The first two are located at 330 cm^{-1} and 379

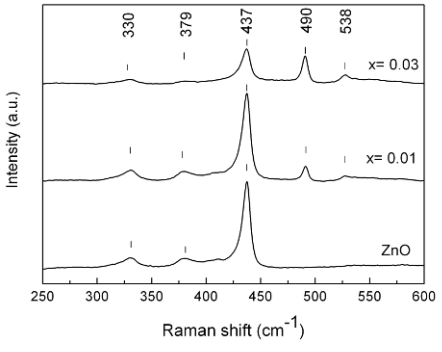

Figure 4. Raman spectra of ZnO pure and of $Zn_{1-x}Co_xO$ ($x = 0.01$ and $x = 0.03$) powders.

cm^{-1} and are assigned to the second-order vibration mode and transverse-optical mode, respectively. The third peak at about 437 cm^{-1}, which is the strongest one, can be assigned to the high frequency branch of the E_2 mode, which is the strongest mode for wurtzite crystalline structure. This peak weakens and becomes much broader with increase of the Co content. The broadening of the E_2 modes reflects the deterioration of the host lattice by the distortion of local atomic arrangement around the magnetic impurities.

Compared with the pure ZnO sample, the Raman spectra of $Zn_{1-x}Co_xO$ have two supplementary peaks. The peak at 490 cm^{-1} is assigned to the most probable impurity phase, Co_3O_4 [22]. This impurity phase wasn't observed in XRD measurements, possibly due to its relatively low concentration, which makes it difficult to detect. For this phase, the diffraction peaks are most probably not sufficiently intense to be distinguished from the background noise level. The peak observed at 538 cm^{-1} is due to the presence of host lattice defects such as oxygen vacancy and Zn interstitials [23, 24]. It could be observed that the peak intensity increases with the increase in Co doping which suggests that the concentration of the structural defects also increases.

The Raman spectra for our samples, in the extended range, don't show any infrared absorption bands near 3500 cm^{-1}. This absorption band corresponds to the hydrogen content in ZnO, in the form of hydroxide ions OH^-, which could influence the electrical properties of the powders [25].

Information concerning the magnetic behaviour of our samples could be obtained using the EPR spectroscopy. As an example, the EPR spectra measured at $T = 20$ K for $Zn_{1-x}Co_xO$ ($x = 0.01$, 0.03) samples are presented in Fig. 5. These spectra are typical for the isolated Co^{2+} ion in powders [26]. The cobalt atoms substitute the zinc atoms and the neutral charge state is Co^{2+} (a $3d^7$ configuration). Co^{59} has $I = 7/2$ which gives rise in single crystals to an eight line hyperfine pattern. For $Zn_{1-x}Co_xO$ powder samples, the EPR data represent an average spectrum over all field orientations. The corresponding EPR spectra are compose of two lines near 1500 G and 3000 G (Fig 5) which correspond to the effective $g_{zz} = 4.4$ and $g_{xx} = 2.27$, suggesting that the symmetry is axially distorted. The absence of the hyperfine structure could be due to an increasing number of randomly distributed defects, which enhances disorder of the crystalline field at Co^{2+} sites [27]. The experimental EPR spectra of our samples can be observed up to a temperature of 200 K and then disappear due to very short spin-lattice relaxation time which considerably broadens the lines.

Both the bulk and Co_3O_4 nanoparticles show, in the temperature range 30 – 300 K, only a single EPR line with

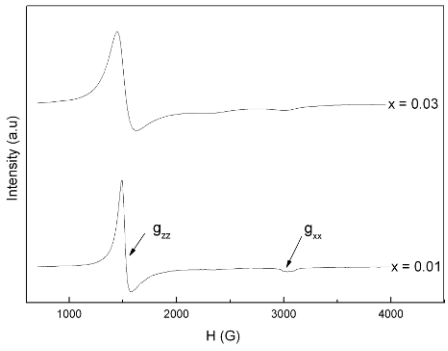

Figure 5. X-band EPR spectra of $Zn_{1-x}Co_xO$ powders with $x = 0.01$ and $x = 0.03$ at $T = 20$ K.

Lorentzian shape and $g = 2.19$ [28]. Nanocrystalline Co_3O_4 samples obtained at various calcination temperatures and with various concentrations of structural additives were also investigated by EPR [29]. For a calcinated temperature of 773 K, the EPR spectrum consists of a broad Lorentzian line centred at $g = 2.52$ and with the line width of 1810 Gs. An additional spectrum at $g_{eff} = 3.5$ having a hyperfine structure was also identified. From the inspection of Fig. 5 one can see that no such EPR absorption lines appear in $Zn_{1-x}Co_xO$ powders. Like the above mentioned XRD results, the presence in our samples of the Co_3O_4 secondary phase cannot be identified by EPR, probably due to its very low concentration.

Direct information about the magnetic state of $Zn_{1-x}Co_xO$ powders can be obtained from the variation of EPR spectrum integral intensity, I, with the temperature [30]. The intensity $I(T)$ is proportional to the spin susceptibility of the paramagnetic species taking part in resonance. In Fig. 6 we show the temperature dependence of $1/T$ for $Zn_{1-x}Co_xO$ with $x = 0.01$ and $x = 0.03$. $I(T)$ was obtained by the double integration of the corresponding EPR spectra.

In the high temperature limit, the variation of $I(T)$ can be described by

$$I(T) \sim \frac{C(x)}{T - \Theta(x)}, \qquad (1)$$

where C is the Curie constant and Θ the Curie-Weiss temperature, both being dependent on the dopant concentration, x. The numerical value of Θ is obtained from the linear extrapolation of the high temperature part of $1/I$ as indicated by the straight line in Fig. 6. The evaluated Θ values are 60 K and 53 K for the samples with $x = 0.01$ and $x = 0.03$, respectively. The positive sign of the Curie-Weiss temperatures indicate that the Co ions are ferromagnetically coupled in our samples. By following the

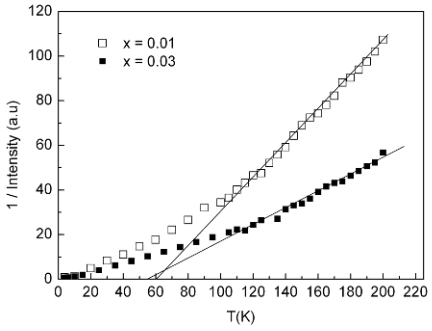

Figure 6. Temperature dependence of the inverse of EPR integral intensity, 1/*I*, corresponding to $Zn_{1-x}Co_xO$ (x = 0.01, 0.03) powders.

same procedure of Θ evaluation, a very weak ferromagnetism was identified in epitaxial (Zn, Co)O layers [30] while Co doped ZnO nanowires show a paramagnetic behaviour [31].

A detailed analysis of the temperature dependence of the integral intensity of the EPR spectra could imply, beside the term described by Eq. 1, two additional contributions arising from the presence of Co pairs and clusters [32]. Co^{2+} exchange pairs were observed by EPR in single-crystalline $Zn_{1-x}Co_xO$ thin films in the very low doping regime, x = 0.03 [33]. If Co pairs could be formed at higher doping concentrations, those Co ions would not be expected to contribute to the EPR spectrum representing the isolated impurities [34]. A careful analysis of our EPR spectra does not show any signature corresponding to Co pairs and therefore, we did not include in Eq. 1 the specific term corresponding to the Co pairs. Moreover, we also did not take into the consideration the contribution due to the Co clusters since they are more likely to appear for higher x as compared with our concentration range. Typical EPR spectra of metallic Co clusters, probably located at the grain boundaries, were identified in ZnCoO thin epitaxial films with high cobalt concentration, x = 0.3 [35, 36]. In our EPR spectra corresponding to $Zn_{1-x}Co_xO$ (x = 0.01, 0.03) powders there are no extra lines which could be attributed to Co clusters (Fig. 5). Since we cannot detect the presence in our samples of metallic Co clusters by XRD or Raman spectroscopy, further electron microscopy analysis is underway in order to fully understand if such clusters are formed inside the crystalline structure of the samples.

We also plan to calibrate the EPR line intensity by comparison against a spin standard in order to analyze the Curie constant with respect to possible missing spins that might belong to unobserved magnetic structures. From Fig. 6, one could think about the possible presence of a phase transition from a ferromagnetic to a paramagnetic behaviour near 110 K. The mechanism behind this transition is still unclear and needs further investigations. The analysis of the temperature dependence of the EPR line width in $Zn_{1-x}Co_xO$ (x = 0.01, 0.03) powders was already reported [37].

When assigning the origin of FM we have to consider the possibility that the secondary phase formation is responsible. Raman investigation reveals the occurrence of Co_3O_4 impurity phase in our samples. It is an antiferromagnetic compound, with low Neel temperature, in which the super exchange coupling prevails between the nearest-neighbor Co atoms through oxygen atoms [28]. Thus, this impurity phase most likely is not the source of FM. Consequently, the observed FM in $Zn_{1-x}Co_xO$ (x = 0.01, 0.03) powders should originate from other complex mechanisms.

In what follows, we refer to the investigations where it was found that interfaces between Co_3O_4 and ZnO are involved in the observed FM in (Zn, Co)O systems [38, 39].

Here, the FM seems to be related to the surface reduction of the Co_3O_4 nanoparticles that are surrounded by the CoO-like shell [38]. Based on these results, we could assume that the observed FM in our $Zn_{1-x}Co_xO$ (x = 0.01, 0.03) powders can be ascribed to the formation of interfaces between two dissimilar valence ions i.e., Co^{3+} ions from Co_3O_4. (formula unit AB_2O_4, A=Co^{2+}, B=Co^{3+}) and incorporated Co^{2+} ions. In another words, the presence of the interfaces between incorporated Co^{2+} ions and Co^{3+} ions is responsible for the observed FM via a possible double-exchange mechanism. The same mechanism was used to account for the room temperature ferromagnetism evidenced in Co doped ZnO nanorods with hidden secondary phases [40]. The presence of oxygen vacancies, as determined from Raman investigation, could also contribute to achieve an adequate ferromagnetic exchange coupling between the incorporated Co^{2+} ions.

4. Conclusions

In summary, we have reported a comprehensive structural and magnetic study on $Zn_{1-x}Co_xO$ powders with x = 0.01 and 0.03. SEM measurements show that the particles size increases with the concentration of the dopant while the presence of a Co_3O_4 secondary phase was evidenced by Raman spectroscopy in both samples. From the analysis of the temperature dependence of the EPR integral intensity, the Curie-Weiss temperatures were evaluated and a ferromagnetic behaviour was evidenced for the investigated samples.

Acknowledgment

At National Institute for Research and Development of Isotopic and Molecular Technologies, Cluj Napoca, Romania, this work was supported by CNCSIS-UEFISCSU, project number PNII-IDEI Nr. 4/2010, code ID-106.

References

[1] G. A. Prinz, Science 282, 1660 (1998)
[2] S. A. Wolf, D. D. Awschalom, R. A. Buhrman, Science 294, 1488 (2001)
[3] T. S. Herng, S. P. Lau, S. F. Yu, J. S. Chen, K. S. Teng, J. Magn. Magn. Mat. 315, 107 (2007)
[4] W. Chen, L. F. Zhao, Y. Q. Wang, J. H. Miao, S. Liu, Z. C. Xia, S. L. Yuan, Solid State Comm. 134, 827 (2005)
[5] J. W. Quilty, A. Shibata, J. Y. Son, K. Takubo, T. Mizokawa, H. Toyosaki, T. Fukumura, M. Kawasaki, Phys. Rev. Lett. 96, 0272021 (2006)
[6] C. Song et al., Phys. Rev. B 73, 024405 (2006)
[7] P. Sati et al., Phys. Rev. Lett. 96, 017203 (2006)
[8] G. Lawes, A. S. Risbud, A. P. Ramirez, R. Seshadriet, Phys. Rev. B 71, 0452011 (2005)
[9] M. Bouloudenine, N. Viart, S. Colis, J. Kortus, A. Dinia, Appl. Phys. Lett. 87, 052501 (2005)
[10] T. Dietl, H. Ohno, F. Matsukara, J. Cibert, D. Ferrand, Science 287, 1019 (2000)
[11] J. M. D. Coey, M. Venkatesan, C. B. Fitzgerald, Nat. Mater. 4, 173 (2005)
[12] K. R. Kittilstved, J. Zhao, W. K. Liu, J. D. Bryan, D. A. Schwartz, D. R. Gamelin, Appl. Phys. Lett. 89, 062510 (2006)
[13] W. K. Liu, G. M. Salley, D. R. Gamelin, J. Phys. Chem. B 109, 14486 (2005)
[14] K. R. Kittilstved, W. K. Liu, D. R. Gamelin, Nat. Mater. 5, 291 (2006)
[15] K. U. Tabata, T. Kawai, Appl. Phys. Lett. 79, 988 (2001)
[16] H. T. Lin, T. S. Chin, J. C. Shih, Appl. Phys. Lett. 85, 621 (2004)
[17] S. C. Wi et al., Appl. Phys. Lett. 84, 4233 (2004)
[18] S. Zhou, K. Potzger, G. Zhang, F. Eichhorn, W. Skorupa, M. Helm, J. Fassbender, J. Appl. Phys. 100, 114304 (2006)
[19] X. Z. Li, J. Zhang, D. J. Sellmyer, Solid State Commun. 141, 398 (2007)
[20] C. Sudakar, J. S. Thakur, G. Lawes, R. Naik, V. M. Naik, Phys. Rev. B 75, 054423 (2007)
[21] M. Opel, K. W. Nielsen, S. Bauer, S. T. B. Gönnenwein, R. Gross, J. C. Cezar, D. Schmeisser, J. Simon, W. Mader, Eur. Phys. J. B 63, 437 (2008)
[22] J. Hays, K. M. Reddy, N. Y. Graces, M. H. Engelhard, V. Shutthanandan, M. Luo, C. Xu, N. C. Giles, C. Wang, S. Thevuthasan, A. Punnoose, J. Phys-Condens Mat. 19, 266203 (2007)
[23] J. B. Wang, G. J. Huang, X. L. Zhong, L. Z. Sun, Appl. Phys. Lett. 88, 252502 (2006)
[24] B. C. Cheng, Y. H. Xiao, G. S. Wu, L. D. Zhang, Appl. Phys. Lett. 84, 416 (2004)
[25] N. Volbers, H. Zhou, C. Knies, D. Pfisterer, J. Sann, D. Hofmann, B. Meyer, Appl. Phys. A-Mater. 88, 153 (2007)
[26] B. M. Weckhuysen, An A. Verberckmoes, M. G. Uytterhoeven, F. E. Mabbs, D. Collison, E. de Boer, R. A. Schoonheydt, J. Phys. Chem. B 104, 37 (2000)
[27] S. K. Misra, S. I. Andronenko, K. M. Reddy, J. Hays, A. Punnoose, J. Appl. Phys. 99, 08M106 (2006)
[28] P. Dutta, M. S. Seehra, S. Thota, J. Kumar, J. Phys-Condens. Mat. 20, 015218 (2008)
[29] N. Guskos, J. Typek, M. Maryniak, G. Zolnierkiewicz, M. Podsiadly, W. Arabczyk, Z. Lendzion-Bielun, U. Narkiewicz, Mater. Sci.-Poland 24, 1095 (2006)
[30] N. Jedrecy, H. J. von Bardeleben, Y. Zheng, J. L. Cantin, Phys. Rev. B 69, 041308(R) (2004)
[31] A. O. Ankiewicz, M. C. Carmo, N. A. Sobolev, W. Gehlhoff, E. M. Kaidashev, A. Rahm, M. Lorenz, M. Grundmann, J. Appl. Phys. 101, 024324 (2007)
[32] S. M. Kaczmarek, G. Leniec, J. Typek, G. Boulon, A. Bensalah, J. Lumin. 129, 1568 (2009)
[33] P. Sati, A. Stepanov, V. Pashchenko, Low Temp. Phys.+ 33, 927 (2007)
[34] J. Hays, K. M. Reddy, N. Y. Graces, M. H. Engelhard, V. Shutthanandan, M. Luo, C. Xu, N. C. Giles, C. Wang, S. Thevuthasan, A. Punnoose, J. Phys-Condens. Mat. 19, 266203 (2007)
[35] N. Jedrecy, H. J. von Bardeleben, D. Demaille, Phys. Rev. B 80, 205204 (2009)
[36] H. J. von Bardeleben, N. Jedrecy, J. L. Cantin, Appl. Phys. Lett. 93, 142505 (2008)
[37] O. Raita, A. Popa, D. Toloman, M. Stan, A. Darabont, L. Giurgiu, Appl. Magn. Reson. 40, 245 (2011)
[38] M. S. Martin-Gonzalez et al., J. Appl. Phys. 103, 083905 (2008)
[39] A. Quesada, M. A. Garcia, M. Andres, A. Hernando, J. F. Fernandez, A. C. Caballero, M. S. Martin-Gonzalez, F. Briones, J. Appl. Phys. 100, 113909 (2006)
[40] X. Wang, R. Zheng, Z. Liu, H. P. Ho, J. Xu, S. P. Ringer, Nanotechnology 19, 455702 (2008)